Nat. Hazards Earth Syst. Sci. Discuss., 2, 2681–2707, 2014
www.nat-hazards-earth-syst-sci-discuss.net/2/2681/2014/
doi:10.5194/nhessd-2-2681-2014

Natural Hazards and Earth System Sciences Discussions
Open Access

Paleoclimate and paleoseismic events discovered from the Diexi barrier lake on the Minjiang River, China

X.Q. Wang[1], **Y.R. Li**[2], **Y. Yuan**[1], **Z. Zhou**[1], **and L.S. Wang**[1]

[1]State Key Laboratory of Geohazard Prevention and Geoenvironment Protection (Chengdu University of Technology), Chengdu 610059, China
[2]Taiyuan University of Technology, Taiyuan 030024, China

Received: 16 February 2014 – Accepted: 10 March 2014 – Published: 15 April 2014

Correspondence to: Y.R. Li (li.dennis@hotmail.com)

Published by Copernicus Publications on behalf of the European Geosciences Union.

Paleoclimate and paleoseismic events discovered from the Diexi barrier lake

X.Q. Wang et al.

Abstract

Studies on the formation of the ancient Diexi barrier lake on the Mingjiang River, southwest China, have long been carried out. However, investigations into the correlation between the paleoclimate and paleoenvironment and the paleoseismic events in this area are rarely found in literature. The present study took sediments from the ancient Diexi barrier lake to investigate the paleoclimate, paleoenvironment and paleoseismic events. A drilling at the center of the barrier lake was conducted and the core of about 260 m long was examined. The paleoclimate and paleoenviornment indicators (sporopollen, carbon and oxygen isotope, organic matter, calcium carbonate, granularity) from the sediments have been tested and analyzed, which indicate that there were ten climatic and environmental periods in between 30 000 a BP and 15 000 a BP. The discovered disturbance segments in the core indicate there were at least ten seismic events during that period. The consistency between climate change and seismic event indicates that a strong seismicity is normally accompanied by a climatic variation. This may be a useful supplement for the climate and geohazard prediction for the future.

1 Introduction

The foreign matters caused by rockfall, landslide, debris flow and lava flow often clog a river by forming a barrier on it. Earthquake is normally one of the main causes for rockfall, landslide and mudflow (Huang et al., 2008). The ancient barrier lake refers to the remains formed by such events long time ago. Previous studies about the barrier lake mainly focused on the formation mechanism and stability of the barrier and the environment change with the life of the barrier. Weidinger (1998) investigated the stability of the landslide barriers located at the Himalaya Mountains. Trauth and Strecker (1999) dated the formation time of the landslide barrier lake located at the northwest Argentina. Wassmer et al. (2004) have investigated the landslide barrier lake located at the valley of Rhine in Swiss and the research mainly aimed at the failure mechanism of the barrier. Krivonogov (2005) studied the ice dammed lake located at northern Mongolia and aimed at the formation time of the barrier and the environment during the time when the lake existed. Moreiras (2006) investigated the approximate formation time of the landslide barrier lake located at the Cordon Plata River of Andes center and he considered the clogging event related to seismicities, together with climatic conditions, rock formations and geological structures. Yang et al. (2008) investigated the evolution of the ancient barrier lake in the Diexi area by analyzing the lithology and sediment system. An et al. (2008) considered that the lacustrine deposit of the ancient barrier lake along the Minjiang fault ~~reflect~~ the tectonic activities of the fault. Zhang et al. (2009) investigated the climatic variation associated with the Diexi ancient dammed lake by AMS-^{14}C dating and granulometry. They divided the evolution of the paleoclimate in the research area into three stages: Stage I (40.5–33.4 ka BP) being cold and dry climate; Stage II (33.4–31.7 ka BP) being warm and humid; and Stage III (31.7–31.1 ka BP) being relatively warm and humid. Wang et al. (2005, 2007, 2009) studied the geological environment and climatic evolution by dating the deposits in the Diexi barrier lake and indicated that the barrier lake was formed about 30 000 years ago and disappeared about 15 000 years later with a climatic evolution sequence similar to what has been discovered by Zhang et al. (2009).

On the other hand, studies on the paleoclimate and paleoenvironment were carried out by taking barrier lake sediments to investigate the climate change law. Sun et al. (2001) investigated the paleoenvironmental features of Daihai barrier lake by taking core smples between 12.34 m and 14.18 m in depth (age: 10.5 ka BP). Wu et al. (2001) obtained a function between the total organic carbon and its isotope records in the Xingcuo lake sediments and the corresponding precipitation and temperature. Shen et al. (2005) investigated the ancient vegetation environment in Ruoergai basin with sporo-pollen analysis. By sampling from the outcrops, Dan et al. (2002) indicated that the paleoclimate in Diexi area expeiernced an evolution of drought-humectation-drought.

NHESSD
2, 2681–2707, 2014

By testing the sediments in Sant Arcangelo Basin, Moretti et al. (2007) indicated that the formation of the inner deformation of the sediments was caused by earthquakes. Wang et al. (2010) attributed the wave-like structures of the sediments in Diexi ancient barrier lake to earthquakes. Sims (1975) concluded that the wave-like structures of barrier lake sediments may develop in the following cases: the lake being close to the active tectonic zone in the contemporary age; sediments being prone to liquefaction; the wave-like structure of the sediments being similar to the structures formed by the earthquake vibration test; the deformational scale of the sediments being small and normally constrained by the lake boundaries; and the deformational structures being limited to a single stratum by relative horizontal layers.

As above, studies about the Diexi barrier lake so far mainly focused on the morphology of the sediments exposed and the environmental indicators in the sediments. However, researches on the correlation between the paleoclimate and paleoenvironment and the paleo-seismic events in this area are rarely found in literature. The present study takes the sediments of the ancient Diexi barrier lake to investigate the paleoenvironment and paleo-seismic events. A core drilling with entire profile sampling was conducted at the center of the Diexi barrier lake, Tuanjie and Jiaochang Villages. The environmental information (sporo-pollen, carbon and oxygen isotope, organic matter, calcium carbonate, granularity) in the sediments have been obtained. Based on this, ten climatic and environmental periods and ten disturbance sections with wave-like structure along the drill hole are interpreted. It is found that there is a close correlation between the paleoclimatic evolution and the paleo-seismic events.

2 Geological background

The research area is located at northwestern Sichuan Plateau at the western edge of Tibetan Plateau formed by the crush and convergence of the Indian Plate and the Eurasian Plate. And the region crosses the Alpine valley region in the transition between the northwestern Sichuan plate and the Sichuan basin, where the wellknown "north-south earthquake tectonic zone" is located. The region is surrounded by three tectonic plates: the Qinghai-Tibet plate, the Yangzi plate and North Chinese plate. The action of the Indian plate, the Pacific plate and the Eurasian plate makes the structure of this area complex. Revolving tectonic systems are widely spread in the Minjiang River regions. The Jiaochang formation with a mountain shaped arcuate structure is of several hundred meters wide (Fig. 1).

The Diexi ancient barrier lake is located in the deep V-shaped gorge region of the Minjiang River (Fig. 2), where mountains are high, the gorge is deep and the river current is fast with an average water surface gradient of about 10.3 %. The thickness of the sediment in the middle of the barrier lake near Tuanjie Village and Jiaochang is about 200 m. The age of the sediments at the bottom is about 30 000 years and that of the top is about 15 000 years old.

The barrier dam is formed by a series of landslides originated from the bank slopes. As shown in Fig. 3, the top elevation of the lake sediments is about 2340 m a.b.s.l. The thickness of the sediments near Tuanjie and Jiaochang Villages is greater than 200 m. In this area, the sediments are of silty clay. At the tail of the barrier lake in Taiping Village (Fig. 2), the particle size is greater, showing a fluvial deposit feature. The sediments in the lake center consist mainly of layered silty sands and clay with clear color alternative variation (Fig. 4). The thickness of the lamina is 2 to 5 cm.

3 Methodology

Four drillings (ZK1, ZK2, ZK3 and ZK4) were carried out in Jiaochang and Tuanjie area, the central part of the ancient Diexi barrier lake. The depth and top elevation of the four drill holes are 52, 84, 48 and 41.7 m, and 2337, 2177, 2231 and 2292 m a.b.s.l., respectively. The drilling core, totally 216 m long were well photographed and recorded. In order to obtain the environmental information recorded in the sediment, soil samples were taken at every 4 m from the core and totally 53 samples were collected. Each sample was divided into three parts for spore-pollen and the organic matter testing to extract the climatic information during the process of sediment depositing. In addition, 108 soil samples were taken from the core at every 2 m. Each sample was divided into three parts for testing carbon and oxygen isotope, calcium carbonate and particle size distribution, respectively. Dating test was carried out on the core at the soleplate altitude and the top level for determining the sediment formation and extinction time.

All tests were carried out according to ~~national/international~~ standards. The ~~spore-pollen~~ tests followed SY/T 5915-2000; the stable carbon and oxygen isotope tests were based on SY/T 5915-2000; organic matter tests were according to ~~GB 9834-88~~; soil carbonate was based on calcium carbonate tests ~~GB 9835-88~~; particle size distribution followed GB/T50123-1999; and dating tests were according to AMS-^{14}C.

4 Results

4.1 Paleoclimatic indicators

Totally, 12 532 sporo-pollens of 46 kinds are identified from the tests. The content distribution of sporo-pollen along the elevation is shown in Fig. 5. The arboreal sporo-pollen occupies the dominant content of about 59.9–89.1 % with an average of 76.2 %. Shrubby and herbaceous sporo-pollen is the second with the content of 6.7–36.9 % and average of 16.9 %. Ferny sopre and algous sporo-pollen ranks the third with the content of 0.9–17.0 % and average of 6.9 %. The arboreal pollens mainly include pinus, cupressaceae and quercus with little picea/abies, tsuga, ulmus, betula, juglans, tilia and carya. The shrubby and herbaceous pollens include corylus, ephedra, ericaceae, artemisia, chenopodiaceae, gramineae, liliaceae and cyperaceae. The ferny spore and algous pollens include polypodiaceae and concentricystis.

As shown in Fig. 6, the maximum value of δ^{13}C is 0.66 and the minimum is −7.35, with an average of −0.43. The maximum value of δ^{18}O is −7.44 and the minimum is −11.72, with an average of −9.42. The ratio of δ^{13}C to δ^{18}O ranges from 0.77 to

NHESSD
2, 2681–2707, 2014

−0.08, with an average of 0.05. It is noted from Fig. 6 that both $\delta^{13}C$ and $\delta^{18}O$ shows the similar variation pattern along the elevation.

In the entire elevation profile, the maximum value of the organic matter content is 1.57 % and the minimum is 0.17 %, with an average of 0.68 % (Fig. 7). According to the variation of the content, the whole profile can be divided into 11 segments (Segment I through XI). As shown in Fig. 8, the maximum content of the calcium carbonate ($CaCO_3$) is 187.04 g kg^{-1} and the minimum is 58.66 g kg^{-1}, with an average of 141.49 g kg^{-1} in the entire elevation profile. According to the variation of the content of $CaCO_3$, 15 segments can be identified along the elevation profile.

The mean particle size, d_{50}, is presented in Fig. 9 along the elevation. The maximum value of the mean particle size is 0.071 mm and the minimum is 0.002 mm, with an average of 0.013 mm. The distinct variation of d_{50} divides the elevation profile into 11 segments. Through the dating according to the method of AMS-^{14}C, the year at 2094 m a.b.s.l. is 30 830 a BP and that at 2306 m is 16 902 a BP.

4.2 Disturbance segments in the drilling core

Through visual examination of the drilling core, 10 segments are identified as they show disturbance structures as shown in Fig. 10. These disturbed segments typically have the following features: (1) wavy and wrapping structure is popular; (2) the laminas vary in thickness; and (3) the disturbed structure is sandwiched by the neighboring upper and lower horizontal layers.

As shown in Fig. 11a, the wrapping structure is kind of structure formed by the flow of seismic liquefaction under an unconsolidated condition (Sims, 1975). Fig. 11b presents a flame structure in a single layer, which is confined by horizontal stratification at the top, indicating a younger lacustrine deposit after the disturbance. This kind of disturbance exposed in the drilling core and outcrop is thought to be products of earthquakes vibration, which liquefies the unsolidified lacustrine sedimentation.

NHESSD
2, 2681–2707, 2014
Paleoclimate and paleoseismic events discovered from the Diexi barrier lake
X.Q. Wang et al.

Title Page
Abstract | Introduction
Conclusions | References
Tables | Figures
◀| |▶
◀ ▶
Back | Close
Full Screen / Esc
Printer-friendly Version
Interactive Discussion

5 Discussion

It is well known that the sporo-pollen is one of the paleontology indicators which are used for climate proxies. Plants such as pinus, cupressaceae and chenopodiaceae indicate chilliness and drought, while tsuga, quercus, ulmus and corylusplants indicate warmth and humectation. As shown in Fig. 5, arboreal sporo-pollen content is the most pronounced followed by shrubby and herbaceous sporo-pollen. The content of ferny sopre and algous sporo-pollen is relatively low (in most case less than 10 %). According to the variation of sporo-pollen, the whole elevation profile can be divided into nine segments (I to IX) corresponding to nine climates. In each segment, pinus sporo-pollen is the most, followed by quercus or cupressaceae.

Segment I presents a pinus-cupressaceae-quercus-chenopodiaceae sporo-pollen group. According to the average content of pinus, cupressaceae, chenopodiaceae (indicating chilliness and drought), quercus and tsuga (indicating warmth and humectation), the climate in this segment would be cool and mid-humid and the vegetation represents an acerose and broad-leaved forest type.

Segment II is mainly a pinus-quercus-chenopodiaceae sporo-pollen group. The contents of all sporo-pollen are relatively stable. Compared to Segment I, content of pinus and corylus gets increased, that of quercus and larch are obviously decreased, while that of chenopodiaceae and artemisia keep unchanged. This indicates a cold and dry climate and the vegetation is of acerose-leaved forest type.

Segment III presents a pinus-quercus-cupressaceae-chenopodiaceae sporo-pollen group. Content of pinus obviously decreases, while that of cupressaceae and quercus increases sharply, so does larch. As quercus indicates warmth and humectation. Therefore, the climate in this segment is cool and mid-drought and the vegetation is of acerose and broad-leaved forest-grassland type.

Segment IV is mainly a pinus-quercus-cupressaceae-qrtemisia sporo-pollen group. Content of pinus and cupressaceae are basically unchanged. Content of larch and chenopodiaceae obviously decreases, while that of quercus and Tsuga increases

NHESSD
2, 2681–2707, 2014

markedly. This indicates the climate in this segment is of warm and humid feature with acerose and broad-leaved forest-grassland.

Segment V is mainly a pinus-quercus-cupressaceae-chenopodiaceae sporo-pollen group. The content of larch and gramineae increases slightly. The content of quercus and tsuga decreases. This indicates a cold and mid-dry climate with vegetation of acerose and broad-leaved forest type.

Segment VI is a pinus-quercus-corylus-artemisia sporo-pollen group. The content of pinus and cupressaceae increases, while that of chenopodiaceae, quercus and tsuga decreases markedly. This indicates a climate of warm and humid feature with vegetation of acerose-leaved forest type.

Segment VII is a pinus-quercus-chenopodiaceae sporo-pollen group. The content of pinus increases, while that of quercus increases, indicating a cold and mid-humid climate with vegetation of forest-grassland type.

Segment VIII is a pinus-quercus-cupressaceae-corylus-gramineae sporo-pollen group. The content of pinus decreases, while that of quercus increases, indicating a climate of cool and mid-drought feature with vegetation of acerose and broad-leaved forest-grassland type.

Segment IV is mainly a pinus-quercus-quercus-corylus-chenopodiaceae sporo-pollen group. The content of pinus slightly increases, while that of quercus obviously decreases, indicating a cold and dry climate with vegetation of forest type.

The climates in the above-mentioned nine segments exhibit alternate warm-humid and cold-dry climates and alternate vegetation types (forest-grassland type in Segment III, IV, VII and VIII and forest type in Segments I, II, V, VI and IX).

Refering to the study by Chen et al. (2000) on open freshwater lakes, we consider that the high value of δ^{13}C indicates warm climate, while the low value of δ^{13}C means cold climate. On the other hand, the high value of δ^{18}O indicates cold climate, while the low value means humid climate. As shown in Fig. 6, the value of δ^{13}C and δ^{18}O, and their ratio fluctuates with elevation. According to the variation feature of $\delta^{13}C/\delta^{18}O$, the entire elevation profile is differentiated into 13 segments, each representing a climate

NHESSD
2, 2681–2707, 2014

type. Segments I, II, III and X indicate humid and others are dry. Additionally, Segments I, II, IV and V reflect typical cold ~~climate.~~ In general, the upper part of the profile expeirenced somewhat warm and dry ~~climate,~~ while the lower expeirenced relatively cold and humid climate.

The organic matter represents the enrichment of humus in soils, which is generally caused by bioorganic actions. The high percentage of the organic matter not only illustrates the accumulation of the humus, but also indicates a humid condition during the formation of soil and an active process of bioorganic action. A warm and humid climate favors luxuriant growth of vegetations, which is beneficial to the accumulation of humus. Although the content of the organic matter in the stratum would be affected by the decomposition of the organic matter itself, the content measured today is still reflect the biomass values at that time. According to the variation of organic matter content in Fig. 7, the elevation profile can be differentiated into 11 segments.

Based on studies on contemporary lakes, Wang (1991) indicated that a close relationship exists between the sedimentation of calcium carbonate and the climate and environment, as the content of calcium carbonate in the sediments reflects the paleoclimatic features in the process of forming sediments. Generally, the high $CaCO_3$ content represents a cold and dry climate, while the low represents a humid climate. According to this variation of $CaCO_3$ content in Fig. 8, the elevation profile can be differentiated into 15 segments. Segments I and II are relatively warm and humid, while Segments IX, X and XIV are somewhat cold and dry.

The Diexi barrier lake is an open and drained lake and its sediments stem from materials at upstream of the Minjiang River. The granularity test indicates that the sediments are mostly silty clay, clayey silt and sandy silt. The coarse grain represents plentiful rainfall, humid climate and well hydrodynamic conditions, while the fines represent less rainfall, dry climate and weak hydrodynamic conditions (Chen et al., 2003). As shown in Fig. 9, the average particle sizes exhibit strong fluctuation along the elevation. The variation in the lower portion of the profile is relatively small, while that in the upper is relatively large. According to the granularity, the entire profile can be differentiated

NHESSD
2, 2681–2707, 2014

Title Page
Abstract | Introduction
Conclusions | References
Tables | Figures
◀| |▶
◀ ▶
Back | Close
Full Screen / Esc
Printer-friendly Version
Interactive Discussion

into 11 segments. Segments I, V, VII, IX and XI indicate relatively humid climate, while Segments II, III, IV, VI VIII and X are relatively dry.

Through combining the abovementioned individual climatic indicator and the dating results, Fig. 12 and Table 1 are got to summarize and delineate the paleoclimatic history in the Diexi area. Totally, 10 climate and environment segments are identified. From about 30 830 a BP till 26 916 a BP, the Diexi area ~~is~~ covered by forest vegetation and the climate changed from warm-humid to hot-humid. Since 26 916 a BP, the temperature became lower and the vegetation ~~is~~ of forest-grassland type. From about 22 872 a BP, the climate changed to be warm-dry and hot-dry with forest vegetation in this area. After that a cold climate came and lasted for about 1600 years (from 18 531 a BP to 16 902 a BP) and the vegetation was forest-grassland type. Since 16 902 a BP through 14 992 a BP the temperature got increased. The whole profile shows a cyclic evolution of climate from warm-humid to cold-dry.

Comparing the paleoclimate segments in Fig. 12 and Table 1 and the disturbance zones in Fig. 10, there is a good correlation between the climatic and environmental changes and the earthquake events. It is inferred that strong earthquake is usually accompanied by climate change. In other words, the atmosphere the climate relies on and the rock cycle the earthquake action relies on are closely associated. Base on the prelimary results from this study, we are considering that the climate change and geology environmental evolution of the eastern edge of Tibetan Plateau may proceed cyclically at an interval of about 15 000 years, and the climate ~~chage~~ was accompanied by seismic event. For detailing this argument, further study is demanded to decipher the inner correlations between the climate change and earthquke event.

6 Conclusion

The present study focuses on the Diexi barrier lake in the Minjiang River, which is located in a complex geological region. Drilling and sampling were conducted in the center of the barrier lake. Climatic indicators were examined through an elevation profile from 2090 m to 2330 m a.b.s.l. to recover the paleoclimate in this area. Based on the foregoing discussion, main conclusions can be made as follows:

(1) Ten climatic periods have been identified for the Diexi barrier lake area within the time span from 30 000 years ago to 15 000 years ago, based on examination of the climatic indicators, such as spore-pollen, organic matter, carbon and oxygen isotopes, calcium carbonate and particle size.

(2) Ten earthquake-induced disturbance layers in the lake sediments were identified through examination of the drilling core. This indicates that from 30 000 a BP to 15 000 a BP, there were at least ten strong earthquakes in the Diexi area.

(3) The disturbance sections formed by earthquake show good consistency with the climate changes, indicating that the geology evolution and the climate environment change are associated.

Acknowledgements. This study is supported by the National Natural Science Foundation of China (No. 41072230 and 51309176) and Funding of State Key Laboratory of Geohazard Prevention and Geoenvironment Protection (SKLGP2012Z008).

References

An, W., Zhao, J. Q., and Yan, X. B.: Tectonic deformation of lacustrine sediments in Qiangyang on the Minjiang fault zone and ancient earthquake, Seismol. Geol., 4, 980–988, 2008.

Chen, J. A., Wan, G. J., and Tang, D. G.: Modern climate change Erhai Lake sediment grain size and isotopic records, Nat. Sci. Prog., 10, 253–259, 2000.

Chen, J. A., Wan, G. J., and Zhang, F.: Environmental record in lake sediments at different time scales – a case study in sediment grain size, Chinese Sci. Ser. D, 33, 563–568, 2003.

Duan, L. P.: The Ancient Barrier Lake and Geoenvironment, Diexi, Minjiang River, Ph.D. thesis, Chengdu University of Technology, China, 2002.

Duan, L. P., Wang, L. S., and Yang, L. Z.: The ancient climatic evolution characteristic reflected by carbon and oxygen isotopes of carbonate in the ancient barrier lacustrine deposits, Diexi, Minjiang River, The Chinese Journal of Geological Hazard and Control, 13, 91–96, 2002.

Krivonogov, S. K., Sheinkman, V. S., and Mistruykov, A. A.: Stages in the development of the Darhad dammed lake (Northern Mongolia) during the Late Pleistocene and Holocene, Quatern. Int., 136, 83–94, 2005.

Liu, D. S.: Loess and Environment, Peking Science and Technology Press, Beijing, China, 348 pp., 1985.

Moreiras, S. M.: Chronology of a probable geotectonic Pleistocene rock avalanche, Cordon del Plata (Central Andes), Mendoza, Argentina, Quatern. Int., 148, 138–148, 2006.

Rodolfo, K. S. and Umbal, J. V.: A prehistoric lahar-dammed lake and eruption of Mount Pinatubo described in a Philippine aborigine legend, J. Volcanol. Geoth. Res., 176, 432–437, 2008.

Trauth, M. H. and Strecker, M. R.: Formation of landslide-dammed lakes during a wet period between 40,000 and 25,000 yr B. P. in northwestern Argentina, Palaeogeogr. Palaeocl., 153, 277–287, 1999.

Wang, L. S., Yang, L. Z., and Li, T. B.: Evolution mechanism of Jiaochang earthquake landslide on Minjiang River and it s cont rolling, Journal of Geological Hazards and Environment Preservation, 11, 195–199, 2000.

Wang, L. S., Yang, L. Z., and Wang, X. Q.: Discovery of huge ancient dammed lake on upst ream of Minjiang River in Sichuan, China, Journal of Chengdu University of Technology: Science and Technology Edition, 32, 1–11, 2005.

Wang, L. S., Wang, X. Q., and Xu, X. N.: What happened on the upstream of Minjiang River in Sichuan Province 20,000 years ago, Earth Science Frontiers, 14, 189–196, 2007.

Wang, P., Zhang, B., Qiu, W. L., and Wang, J. C.: Soft-sediment deformation structures from the Diexi paleo-dammed lakes In the upperreaches of the Minjiang River, east Tibet, J. Asian Earth Sci., 40, 865–872, 2011.

Wang, S. B., Li, Y., and Xia, X. G.: Magnetostratigraphic Study of Lake Sediments in Jiaochang, Maoxian County, Sichuan, 426 pp., 2006.

Wang, S. M. and Li, J. R.: Lake sediments – effective means to study the history of climate – an example from Qinghai Lake and Daihai Lake, Chinese Sci. Bull., 36, 54–56, 1991.

Wang, X. Q.: The Environment Geological Information in the Sediments of Diexi Ancient Dammed Lake on the upstream of Mingjiang River in Sichuan Province, China, Ph.D. thesis, Chengdu University of Technology, Chengdu, China, 2009.

Discussion Paper | Discussion Paper | Discussion Paper | Discussion Paper |

Wassmer, P., Schneider, J. L., Pollet, N., and Schmitter-Voirin, C.: Effects of the internal structure of a rock-avalanche dam on the drainage mechanism of its impoundment, Flims sturzstrom and Ilanz paleo-lake, Swiss Alps, Geomorphology, 61, 3–17, 2004.
Weidinger, J. T.: Case history and hazard analysis of two lake-damming landslides in the Himalayas, J. Asian Earth Sci., 16, 323–331, 1998.
Weidinger, J. T., Wang, J. D., and Ma, N. X.: The earthquake-triggered rock avalanche of Cui Hua, Qin Ling Mountains, P. R. of China, Quatern. Int., 93–94, 207–214, 2002.
Wu, J. L., Li, S. J., and Wang, S. M.: Modern climatic signals recorded in Xincuo Lake sediments in Zoige Basin, eastern Tibetan plateau, China, Journal of Lake Science, 12, 291–296, 2000.
Yang, W. G.: Research of sedimentary record in terraces and climate vary in the upper reaches of Mingjiang River, china, Ph.D. thesis, Chengdu University of Technology, Chengdu, China, 2005.
Zhang, Y., Zhu, L., and Yang, W., Luo, H., He, D. and Liu J. : High resolution rapid climate change records of lacustrine deposits of Diexi Basin in the eastern margin of Qinghai-Tibet Plateau, 40–30 ka BP, Earth Science Frontiers, 5, 91–98, 2009.
Zhang, Y. S., Zhao, X. T., and Hu, D. G.: An ancient landslide-dammed lake found in the Jinsha River valley near Benzilan, Yunnan, China and its significance, Geological Bulletin of China, 8, 970–975, 2007.
Zhang, X., Walling, D. E., He, X., and Long, Y.: Use of landslide-dammed lake deposits and pollen tracing techniques to investigate the erosional response of a small drainage basin in the Loess Plateau, China, to land use change during the late 16th century, Sediment Sources and Sediment Delivery under Environmental Change, 79, 205–213, 2009.
Zhao, X. T., Qu, Y. X., and Zhang, Y. S.: Discovery of Shigu Paleolake in the Lijiang area, northwestern Yunnan, China and its significance for the development of the modern Jinsha River valley, Geological Bulletin of China, 8, 960–969, 2007.
Zhu, D. G., Meng, X. G., and Zhao, X. T.: Lake-level change of Namco Tibet since the Late Pleistocene and environment information of clay minerals in lacustrine deposits, 10, 300–309, 2004.

NHESSD
2, 2681–2707, 2014

Paleoclimate and paleoseismic events discovered from the Diexi barrier lake

X.Q. Wang et al.

Table 1. The paleoclimatic periods in the study area.

Segment	Elevation of disturbance layer (a.b.s.l.)	Paleoclimate and paleoenvironment			
		Elevation (a.b.s.l.)	Period (a BP)	Climate	Vegetation
10	2321–2313	2323–2333	15 650–14 992	warm-humid	forest
9	2306–2300	2301–2323	16 902–15 650	warm-dry	forest – grassland
8	2291–2288	2290–2301	17 413–16 902	cool-dry	forest – grassland
7	2275–2269	2273–2290	18 531–17 413	cold-dry	forest – grassland
6	2262–2253	2229–2273	21 425–18 531	hot-dry	forest
5	2206–2200	2207–2229	22 872–21 425	warm-dry	forest
4	2193–2189	2174–2207	25 043–22 872	cold-dry	forest – grassland
3	2166–2163	2146–2174	26 916–25 043	cool-dry	forest – grassland
2	2154–2152	2115–2146	29 077–26 916	hot-humid	forest
1	2137–2134	2095–2115	30 830–29 077	warm-humid	forest

NHESSD
2, 2681–2707, 2014

1. Main faults; 2. Boundary of intrusive rock; 3. Syncline; 4. Anticline; 5. Klippe; and 6. Inferred fault

Fig. 1. Regional geology.

NHESSD
2, 2681–2707, 2014

Paleoclimate and paleoseismic events discovered from the Diexi barrier lake

X.Q. Wang et al.

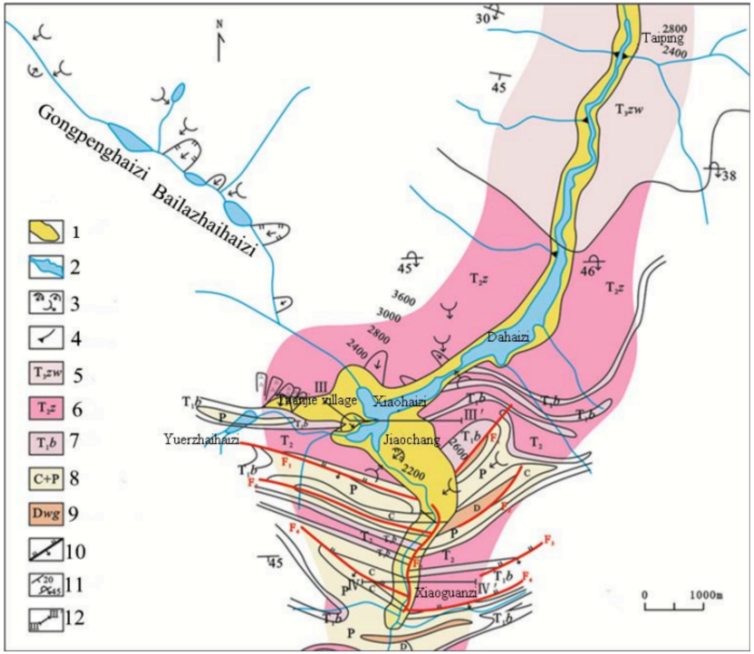

1. The Diexi barrier lake; 2. Barrier lake by the 1933 earthquake; 3. Landslide; 4. Debris flow valley; 5. Zhuwei formation of Triassic; 6. Zagunao formation of Triassic; 7. Bocigou formation of Triassic; 8. Formation of Carboniferous; 9. Weiguan formation of Devonian; 10. Fault; 11. Strike and dip; and 12. Cross section

Fig. 2. Geological map of the Diexi area.

NHESSD
2, 2681–2707, 2014

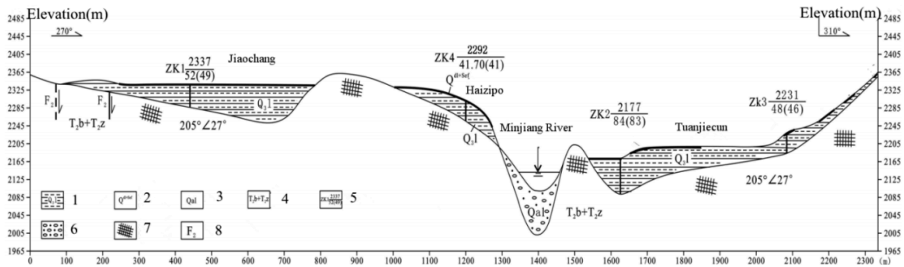

1. lacustrine deposit; 2. Colluvium; 3. Alluvium; 4. Bocigou and Zagunao formation of Triassic;

5. Drilling; 6. Alluvium; 7. Sand slate; 8. Fault

Fig. 3. Typical cross section of the Diexi barrier lake (Section III-III’ in Fig. 2.)

NHESSD
2, 2681–2707, 2014

Fig. 4. Structure of lacustrine sediment in the Diexi barrier lake.

NHESSD

2, 2681–2707, 2014

Paleoclimate and paleoseismic events discovered from the Diexi barrier lake

X.Q. Wang et al.

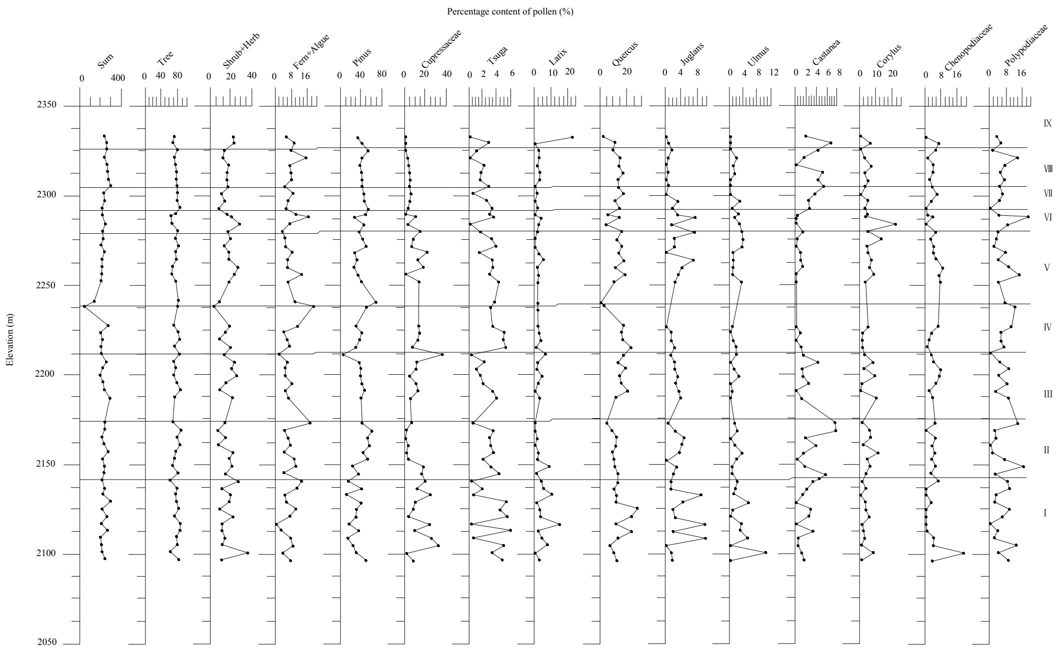

Fig. 5. Pollen and spore schema along the elevation.

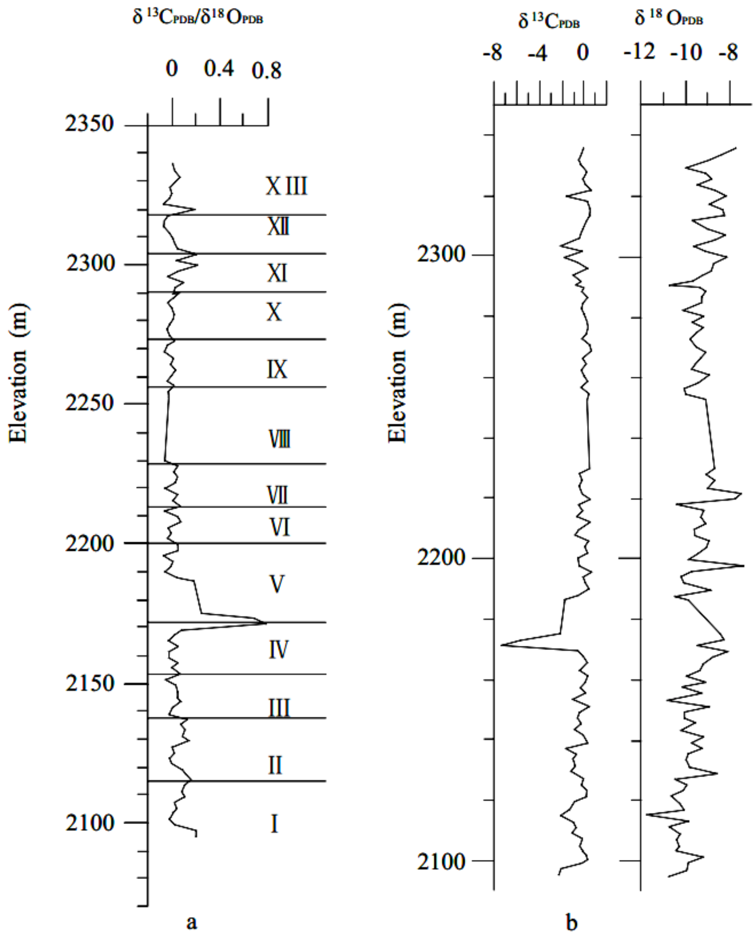

Fig. 6. Carbon and oxygen isotopes: **(a)** ratio of δ^{13}C to δ^{18}O; and **(b)** values of δ^{13}C and δ^{18}O.

NHESSD
2, 2681–2707, 2014

Paleoclimate and paleoseismic events discovered from the Diexi barrier lake

X.Q. Wang et al.

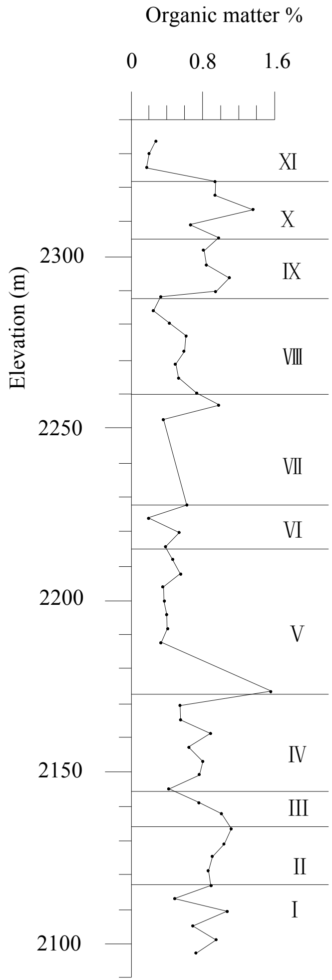

Fig. 7. Average content of organic matter.

NHESSD
2, 2681–2707, 2014

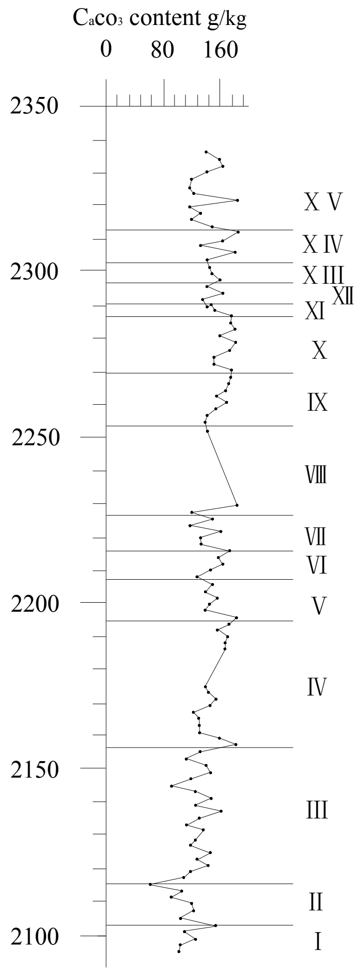

Fig. 8. Content of $CaCO_3$ along the elevation.

NHESSD
2, 2681–2707, 2014

Paleoclimate and paleoseismic events discovered from the Diexi barrier lake

X.Q. Wang et al.

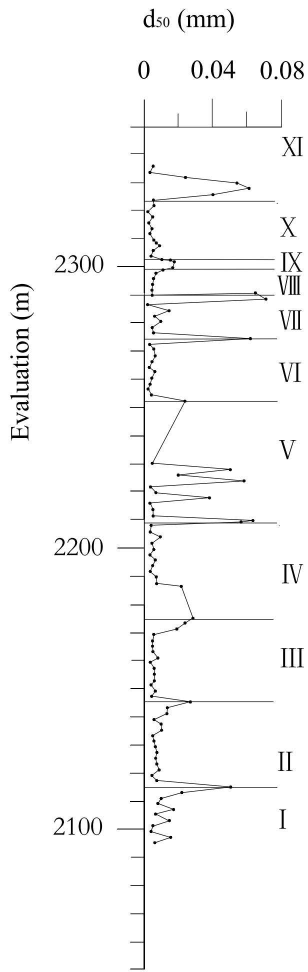

Fig. 9. Mean particle size, d_{50}.

NHESSD
2, 2681–2707, 2014

Paleoclimate and paleoseismic events discovered from the Diexi barrier lake

X.Q. Wang et al.

Fig. 10. Features of disturbance layers in the drilling core.

NHESSD
2, 2681–2707, 2014

Paleoclimate and paleoseismic events discovered from the Diexi barrier lake

X.Q. Wang et al.

Title Page
Abstract | Introduction
Conclusions | References
Tables | Figures
◀| |▶
◀ ▶
Back | Close
Full Screen / Esc
Printer-friendly Version
Interactive Discussion

a

b

Fig. 11. Earthquake-induced disturbance layer in the sediment exposed on an outcrop.

NHESSD
2, 2681–2707, 2014

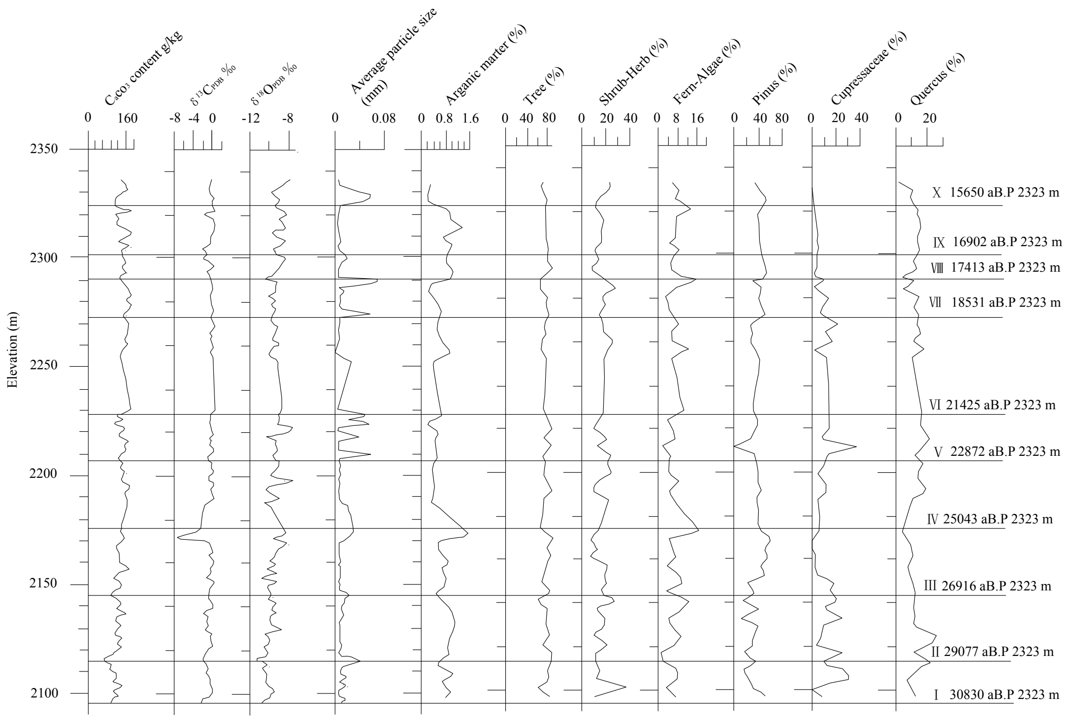

Fig. 12. Delineation of paleoclimate in the study area.

NHESSD

2, 2681–2707, 2014